Volume: 1 Issue: 14 Pages: 107-110

International Journal of Research in Academic World

E-ISSN: 2583-1615
Impact Factor: 4.714

Received: 11/September/2022 Int. J Res. Acad. World. 2022; 1(14):107-110 Accepted: 06/October/2022

X-Ray Study of Brightest Cluster Abell 1664

[*1]BT Tate and [2]AT Kyadampure

[*1]Department of Physics, Balbhim Arts, Science and Commerce College, Beed, Maharashtra, India.

[2]Department of Physics, Sanjeevanee Mahavidyalaya, Chapoli, Maharashtra, India.

Abstract
We present results obtained from 235 ks Chandra data observation of the cool core cluster abell 1664 obtained from Chandra data center. These data were processed with CIAO 4.7 and Chandra CALDB 4.6.7. X-ray imaging of Abell 1664 showed the presence of an possible pair of ellipsoidal cavities along the East and West directions within the central region. Imaging and spectral studies showed the removal of substantial amount of matter from the core of the cluster. We have plotted tricolor map in three different energy bands of X-ray to analyze distribution of ICM this cluster, to investigate extent of the X-ray emission from this cluster, we have generated its surface brightness profile as well as sectoral radial profile reveals that the ICM distribution within this cluster is not isotropic and homogeneous. This radial profile yielded the slope and core radius parameters to be equal to $\beta = 0.51$ and $rc = 11.68$ pixels. Superb spatial resolution capability of Chandra was used to investigate the temperature and metallicity distribution across the cluster Abell 1664 using contour binning technique. We have also prepared tricolor map of optical DSS r-band image image, 2MASS image and X-ray image to see association of ICM in this cluster.

Keywords: Galaxies, cluster, brightest cluster Abell 1664, X-rays

Introduction

It is well known that feedback from AGNs plays an important role in the evolution of hot gas in galaxies as well as galaxies in groups and clusters [1, 2, 3, 4, 5, 6, 7, 8]. In recent time high resolution X-ray observations with the Chandra telescopes have shown that the X-ray-emitting gas from cooling flow galaxies does not cool abruptly from the plasma state to the molecular state, but instead is reheated. The current model is that AGNs in the cluster dominant galaxy are accountable for this reheating, implying a complicated feedback process between the cooling gas and the central galaxy [9]. AGNs also play important roles in adapting the morphologies of the hot gas haloes enclosing individual galaxies, groups and clusters and the formation of cavities and bubbles [10]. These cavities are depressions in X-ray surface brightness filled relativistic plasma and are a effect of the thermal gas being displaced by jets from the central AGN [11]. It is widely approved that mass accretion on to the central massive black hole is the ultimate source of energy for the formation of cavities. Now a day observing facilities at X-ray wavelengths with high resolution have made it achievable to detect such cavities or bubbles of a few to a few tens of kpc size. Clusters of galaxies have give the strongest observational information for the AGN feedback in galaxy clusters. In the majority of systems, these X-ray cavities are found to be associated with radio jets and are spatially coincident with radio bubbles or lobes [3]. Combined X-ray and Radio observations of such systems have indicated that these cavities are augmented by bipolar jets emanating from AGNs located at the center of a CDG [12]. Like radio jets, in many cases, X-ray cavities also seen in pairs [13]. These X-ray cavities are found to be filled with radio emission [14]. Though X-ray cavities have also been detected in groups, the majority of the studies on AGN feedback have been focused on cavity systems seen in the massive and X-ray luminous galaxy clusters, and groups have received less attention. In this paper, we present a detailed analysis of the X-ray data on Abell1664 the brightest cluster galaxy (BCG) in the Abell 1664 cluster is unusually blue to investigate the possibility of the X-ray cavities hosted in this system. We present our analysis of the recent multiple Chandra observations and 2MASS and R-DSS images of the cluster and its core.

Table 1: Global Parameters of Abell 1664

Object Name	Abell 1664
R. A.	13h 3m 41.79s
DEC	-24° 13' 6.0"
Redshift	0.1283
Object Type	Brightest Cluster Galaxy

Observations and Data Preparation

We analyzed the Chandra ACIS-S observations of Abell 1664 in VFAINT mode (ObsID: 7901, 17172, 17173, 17557, 17568) with CIAO 4.7 and Chandra CALDB 4.6.7. All observations were reprocessed from level=1 event file following the standard Chandra reduction threads. lc sigma clip was used to remove high background flares. We combined the observations with the merge obs script so that the total cleaned exposure time is 235 ks. For each observation we created a point spread function (PSF) map. These were combined with the corresponding exposure maps in order to obtain a single exposure-corrected (PSF) map. We then ran the wave-detect task on the merged image in order to detect point sources. Sources were confirmed by eyes and

***Corresponding Author:** BT Tate

then excluded from the further analysis. We used the task re-project event to match blank sky background files to the corresponding event files for all Obs ID. Then they were normalized by the ratio of count rates in the 9-12 keV energy band and further combined in to a single background image.

X-Ray Imaging Analysis

The X-ray peak of this cluster corresponds to (RA, DEC) 13h03m42.5s and-24d14m41.0s, respectively. Optical DSS r-band image image of this cluster on which X-ray contours are overlaid are shown in Figure 1 (left panel), While the association of the X-ray peak with the Brightest Cluster Galaxy (BCG) as shown in its tri-colour image (right panel). This has been derived after appropriate combination of the event files in three different energy band namely, soft (0.5-1 keV, shown in red color), medium (1-2 keV, shown in green) and the hard (2-7 keV, shown in blue). This image clearly reveals that the ICM distribution within this cluster is not homogeneous and isotropic, rather it hosts structures within, and are discussed separately.

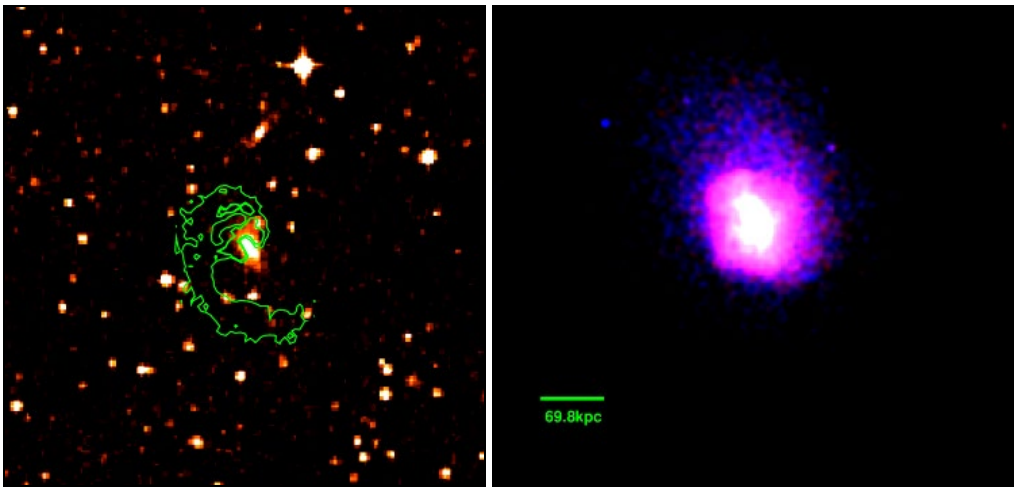

Fig 1: Optical DSS r-band image of the cluster with x-ray contour is shown in left panel while tricolor image (right panel)

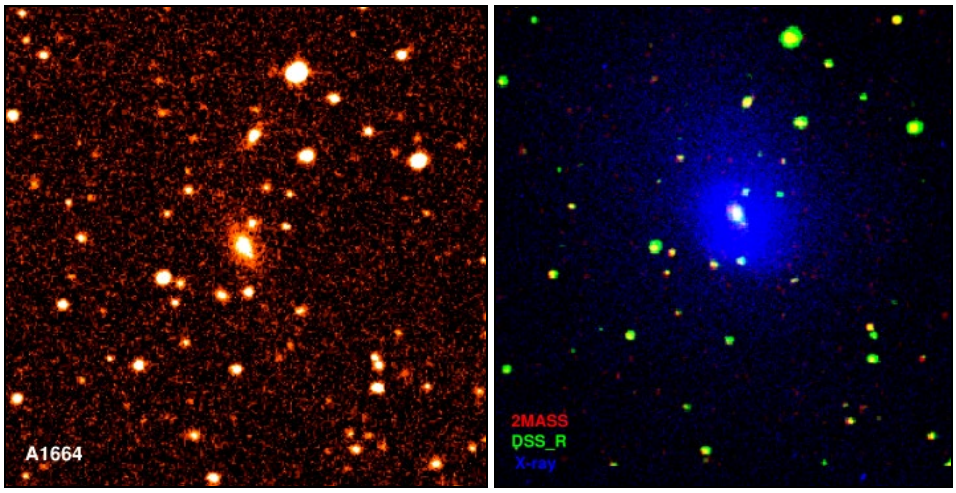

Fig 2: The raw optical DSS r-band image of the cluster is shown in left-hand panel and RGB image of (Red-2Mass, Green-Dss-r and Blue-X-ray image) Abell 1664.

This image has been obtained by combining X-ray emission detected in three different energy bands namely, the soft (0.5-1 keV) shown in red colour, the medium (1-2 keV) green colour and the hard (2-7 keV) blue colour. This image reveals that the ICM distribution is not isothermal, rather it exhibits structures in the spatial distribution of the X-ray emitting gas meaning that various regions emit at different energies. A clear hint for the presence of a spiral pattern due to the disturbance of gas is observed in this figure.

We have also prepared tricolor map of 2Mass (Red), Dss-r (Green)and X-ray image(Blue) observe distribution ICM as shown in Figure 2(right panel).

With an objective to investigate the hidden features within the ICM distribution in this cluster we have derived its unsharp masked image as well as 2D smooth model subtracted residual image. For generating the unsharp mask image we have used the exposure corrected, background subtracted 0.5-3 keV Chandra image of Abell 1664. This image was first smoothed with a lighter Gaussian kernel of width 2σ using aconvolve task within CIAO to suppress the pixel-to-pixel variations of the X-ray emission within the cluster, while preserving the structures on likely scales.

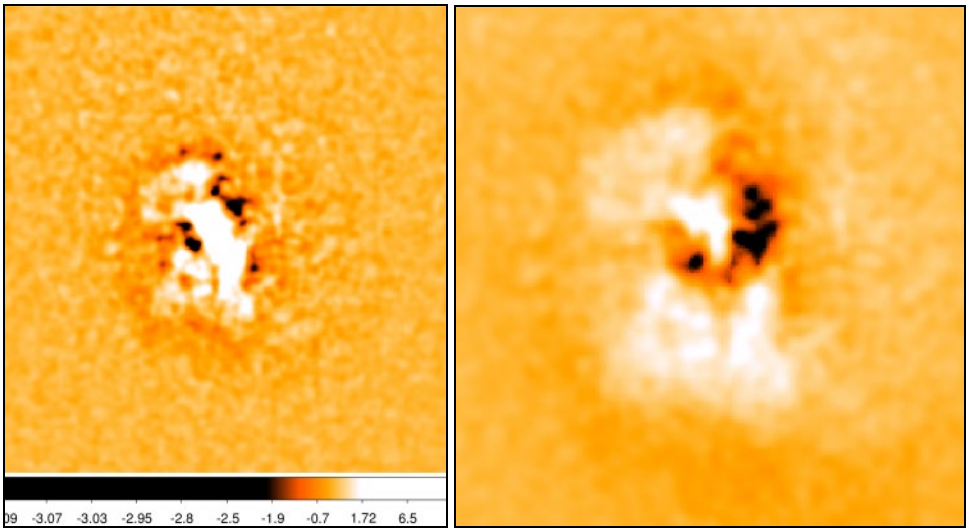

Fig 3: 0.3-3 keV quotient image derived by dividing the original image with the 2D-β model image (left-hand panel), whereas the right-hand panel shows the residual image generated by unsharped mask imaging technique.

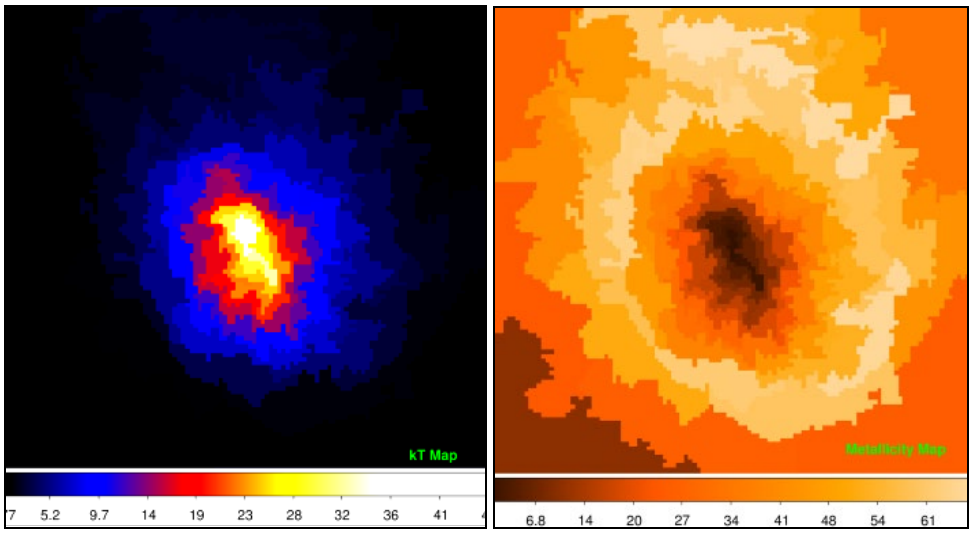

Fig 4: Projected temperature map (left-hand panel) in units of keV and metallicity map (right-hand panel) in units of Z_{Θ} generated by using contour binning technique. Bright and darker shades in the temperature map indicate hotter and cooler regions, respectively, whereas in abundance map, darker shade represent higher metallicity.

The resultant unsharp mask image obtained after subtracting the 10σ Gaussian kernel smoothed image from that with the 2σ is shown in Figure 3(left panel). This figure reveals the presence of a possible cavity in the east and west direction of the image. For further confirmation of these features in unsharp mask image, we create its 2D β-model subtracted residual map. The 2D smooth model of the X-ray emission distribution in this cluster has been computed by fitting ellipses to the isophotes in the cleaned, flare removed, point source detected 0.5-3 keV Chandra image of Abell 1664. The best fit smooth model was then subtracted from the cluster emission to produce its residual image and is shown in Figure 3(right panel). This image clearly confirms all the features apparent in the unsharp mask image exactly matching with 2D-beta model. For comparing its optical counterpart, We have plotted X-ray emission contours in the unsharp masked image on to this DSS image. Notice the extent and structure of the spiral pattern in this figure, which appear to originate from the BCG member of the cluster.

We have generated projected temperature map Figure 4(left-hand panel) in units of keV and metallicity map (right-hand panel) in units of Z_{Θ} by using contour binning technique.

Radial Profile

With an objective to investigate 2D structural and physical properties of the cluster ICM, we compute the azimuthally averaged surface brightness profile of the X-ray emission from this cluster. For this we have extracted 0.5-3 keV X-ray photons from a series of concentric circular annuli centered on the X-ray peak of the cluster extending up to about 120 arc seconds. This was achieved using the ds9 image analysis tool and setting the widths of the concentric annuli such that each annulus contains roughly same number of counts. The background for this analysis was extracted from the blank sky background file. X-ray photons in this energy range were then extracted using the task dmextract within CIAO and were imported to the fitting package sherpa, where we plotted the resultant background subtracted flux of the X-ray emission from this cluster as a function of the radial distance. The resultant surface brightness profile is shown in Figure 5(right panel). To model the distribution of hot gas in this cluster, we fit these data points with one dimensional beta model in applying the Gehrel's $\chi 2$ statistics variance. This model is based on the assumption that the gas in the cluster is in hydrostatic equilibrium and follow the spherical symmetry as assumed by the King's model.

$\Sigma(r)\,\Sigma_0$ Where,

$$\Sigma(r) = \Sigma_0 \left[1 + \left(\frac{r}{r_c}\right)^2\right]^{-3\beta+0.5},$$

rc and β represent the X-ray surface brightness at projected distance r, the central X-ray surface brightness, core radius and the slope parameter, respectively.

The best fit one dimensional beta model to the data points is shown by the dashed line in Figure. 5(left panel) this model fits the data points adequately in the outer region, however, shows excess emission and fluctuations in the surface brightness distribution in the central region. The X-ray emission in the core region exceeds substantially relative to the modeled value, which then decreases systematically in outward direction and is consistent with that observed in several other cool core clusters[15][16]. However, it exhibits a depression in the surface brightness. This beta model fitting exercise yielded the slope and core radius parameters to be equal to β = 0.51 and rc = 11.68 pixels, respectively.

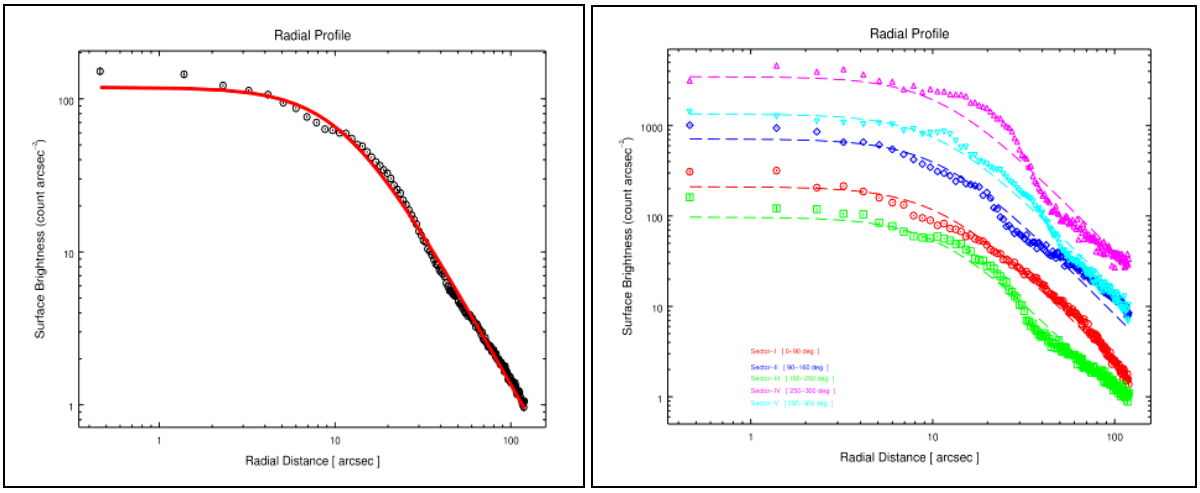

Fig 5: Azimuthally averaged surface brightness profile of Abell 1664(left panel). We also plot similar profiles by extracting X-ray counts from four different wedge shaped regions with their opening angles as described in the figure. For comparison we also show the best fit 1D β-model (dotted lines) for each of the profile. Notice the fluctuations in the surface brightness of ICM. The Projected surface brightness profiles are derived from five different sectors, Sector I (0 ◦-90 ◦), Sector II (90 ◦-160 ◦), Sector III (160 ◦-250 ◦), Sector IV (250 ◦-300◦) and Sector V (295^0-360^0).(right panel)

Conclusion

This conclusions are based on the analysis of the 245 ks Chandra data acquired in five different observing runs (Obs ID 7901, 17172, 17173, 17557, 17568) on Abell 1664, a famous relaxed galaxy cluster at a redshift of 0.1283. This cluster satisfies the quality of being classified as a cool core galaxy cluster and also hosts central dominant system at its core. X-ray imaging analysis of this cluster environment has revealed a pair of possible X-ray deficient region. The temperature structure of the ICM were confirmed through the tri-colour map by appropriate combination of the X-ray flux imaged divided into three different energy bands. The surface brightness analysis yielded the best fitted 1d beta-model parameters as β = 0.51 and core radius =11.67 pixel. The hidden features embedded within this cluster were determined using the systematic imaging analysis and producing its unsharp mask image, two dimensional smooth model subtracted residual map, surface brightness profile, sectoral radial profile clearly reveals that the ICM distribution within this cluster is not homogeneous and isotropic Temperature map of this cluster shows hotter and cooler regions, respectively and metallicity map shows it has higher metallicity.

References

1. Hoeft M, Bruggen M, ApJ, 2004, 617, 896
2. Dunn RJH, Fabian AC, MNRAS, 2006, 373, 959
3. McNamara, B. R. & Nulsen, P. E. J., 2007, ARA&A, 45, 117
4. Diehl S, Statler TS, ApJ, 2008, 687, 986
5. David LP, Jones C, Forman W, Nulsen P, Vrtilek J, O'Sullivan E, Giacintucci S, Raychaudhury S, ApJ, 2009, 705, 624
6. Gastaldello F, Buote DA, Temi P, Brighenti F, Mathews WG, Ettori S, ApJ, 2009, 693, 43
7. Sun M, Voit GM, Donahue M, Jones C, Forman W, Vikhlinin A, ApJ, 2009, 693, 1142.
8. Rasmussen J, Ponman TJ, MNRAS, 2007, 380, 1554
9. Soker N, Pizzolato F, ApJ, 2005, 622, 847.
10. Sun M, Voit GM, Donahue M, Jones C, Forman W, Vikhlinin A, ApJ, 2009, 693, 1142
11. Bˆırzan L, Rafferty DA, McNamara BR, Wise MW, Nulsen PEJ, ApJ, 2004, 607, 800
12. Fabian AC, Sanders JS, Allen SW, Crawford CS, Iwasawa K, Johnstone RM, Schmidt RW, Taylor GB, MNRAS, 2003, 344, L43
13. McNamara BR, Kazemzadeh F, Rafferty DA, Bˆırzan L, Nulsen PEJ, Kirkpatrick CC, Wise MW, ApJ, 2009, 698, 594
14. Wise MW, McNamara BR, Nulsen PEJ, Houck JC, David LP, ApJ, 2007, 659, 1153
15. Clarke TE, Kassim N, Ensslin T, Neumann D, in Engvold O., ed., Proc. IAU Symp. 13, Highlights of Astronomy. Astron. Soc. Pac., San Francisco, 2005, 330.
16. Pandge MB, Vagshette ND, David LP, Patil MK, MNRAS, 2012, 421, 808
17. Pandge MB, Vagshette ND, Sonkamble SS, Patil MK, Ap&SS, 2013, 345, 183.